

SUPPLEMENTAL FIGURES

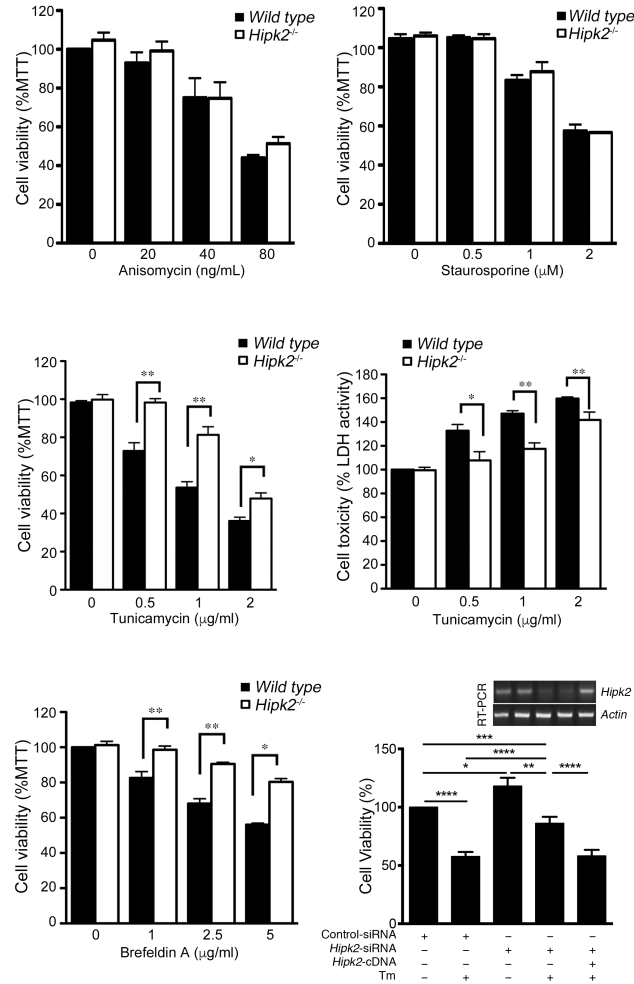


Figure S1. Acute and chronic HIPK2 deficiency protect cells from ER stress-induced cell death, Related to Figure 1

(A-B) Both *wild type* and *Hipk2*^{-/-} MEFs were treated with anisomycin or staurosporine to determine cell death in these cells using MTT assays.

(C-E) *Wild type* and *Hipk2*^{-/-} mouse embryonic fibroblasts (MEFs) were treated with tunicamycin (A, B) or brefeldin A, followed by cell viability assays using 3-(4, 5-dimethylthiazol-2-yl)-2, 5-diphenyltetrazolium-bromide (MTT) to determine the extent of cell death, or cytotoxicity assay using lactate dehydrogenase (LDH).

(F) HEK293 cells were treated with scramble siRNA, *Hipk2* siRNA or *Hipk2* siRNA plus *Hipk2* cDNA for 24 hours, followed by treatment with tunicamycin overnight. Inset: RT-PCR for *Hipk2* mRNA was used to monitor efficiency of *Hipk2* siRNA knockdown.

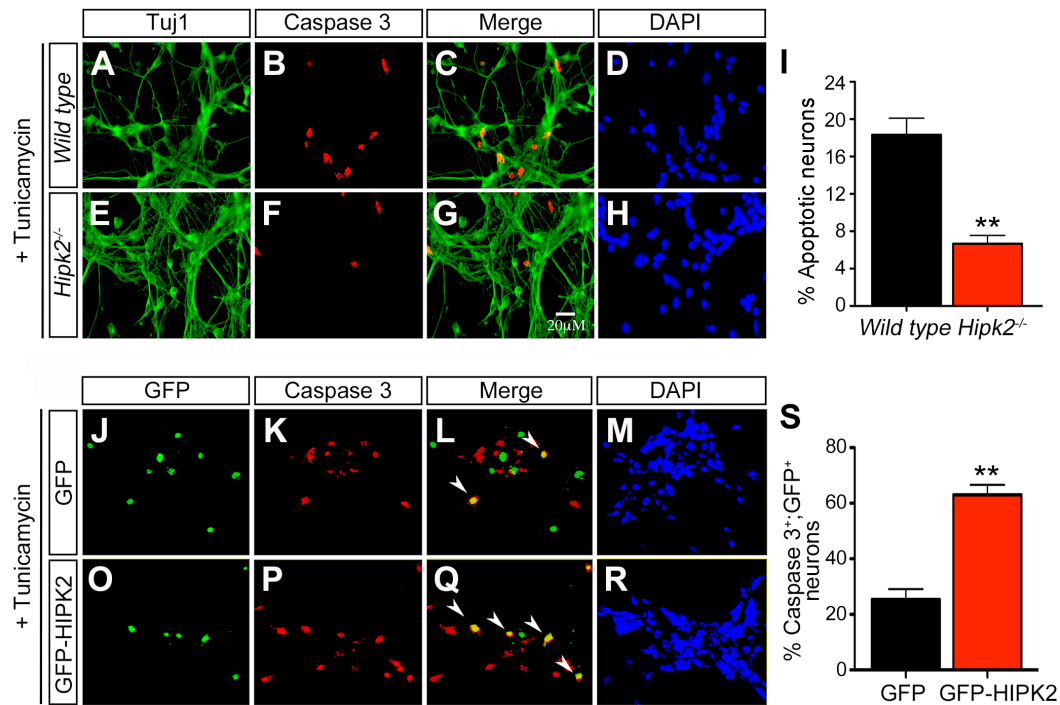


Figure S2. HIPK2 is necessary and sufficient to cause cell death during ER stress, Related to Figure 1

(A-I) Primary cortical neurons (DIV14) from E15.5 *wild type* and *Hipk2*^{-/-} embryos were treated with tunicamycin overnight, fixed in 4% PFA and processed for immunostaining with antibodies that detect Tuj1 (Alexa 488) and activated caspase 3 (Alexa 568). Quantifications of caspase 3 positive neurons are shown in I. Student's *t* test; ** indicate $p < 0.01$. Scale bar in G is 20 μ m, and is applicable to all images in A-H and J-R.

(J-S) *Wild type* cortical neurons expressing GFP or GFP-HIPK2 were treated with tunicamycin overnight and processed for staining for caspase 3, DAPI, and GFP (upper panel) or GFP-HIPK2 (lower panel). Arrowheads show apoptotic neurons positive for GFP and activated caspase 3. The percentage of GFP⁺ apoptotic neurons is shown in S. Data represent mean \pm SEM of three individual experiments. Two-tailed unpaired Student's *t* test; ** indicates $p < 0.01$.

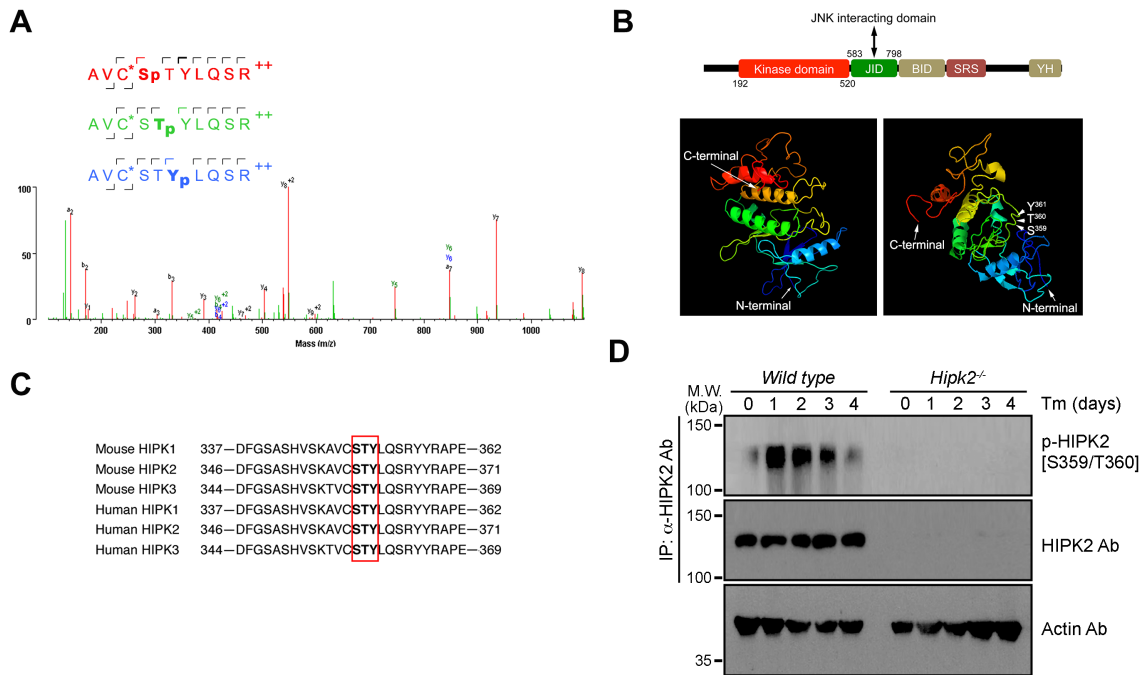


Figure S3. Structural evidence of the highly conserved phosphorylation sites within the activation loop of the HIPK2 kinase domain, Related to Figure 2

(A) Representative LC-MS/MS spectrum of a singly phosphorylated HIPK2 tryptic peptide spanning the S359, T360 and Y361 residues shows overlapping ion series corresponding to phosphorylation at S359, T360 and Y361, highlighted in red, blue and green, respectively. All assigned ion peaks are shown in red.

(B) A schematic diagram of HIPK2, highlighting the kinase domain (amino acids 192-520) and the JNK interaction domain (amino acids 583-798). Using the Phyre² protein structure prediction program, we found that the kinase domain of HIPK2 (amino acids 192 to 520) was structurally analogous to that of inhibitor of kappaB kinase (IKK)(100% confidence in prediction), and that the highly conserved tripartite S359-T360-T361 amino acids in the activation loop of HIPK2 kinase domain were located in a stretch of relaxed residues between short stretches of β -strand structures.

(C) Protein sequence alignment highlights the highly conserved amino acids within the activation loop of HIPK2 kinase domain and the tripartite S359-T360-Y361 amino acids highlighted in a red box.

(D) Protein lysates from the lumbar spinal cord of 3 month-old *wild type* and *Hipk2*^{-/-} mice, treated with tunicamycin for 1-4 days, were used in immunoprecipitation-western blot to detect phosphorylated HIPK2 proteins using p-HIPK2 [S359/T360] Ab.

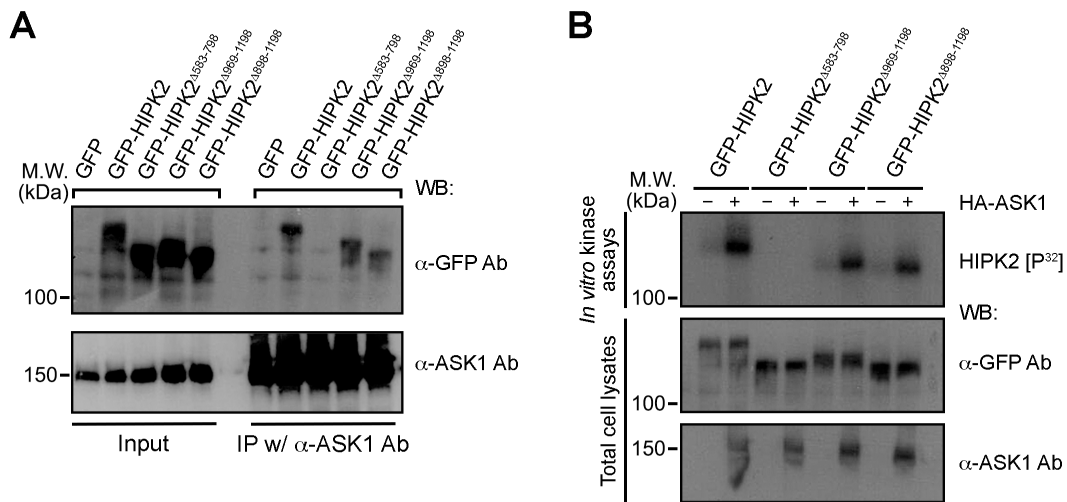


Figure S4. Protein complex formation between ASK1 and HIPK2, Related to Figure 2

(A) Co-immunoprecipitation assays using HEK293 cells that express GFP, GFP-tagged HIPK2 and GFP-HIPK2 with deletion that remove domain between amino acids 583-798, 969-1198 or 898-1198. Protein lysates are incubated with anti-ASK1 antibody and probed with anti-GFP antibody to detect protein complex formation between ASK1 and HIPK2.

(B) Wild type ASK1 promotes HIPK2 phosphorylation in GFP-tagged wild type HIPK2 (GFP-HIPK2), and HIPK2 mutants that lack amino acids 969-1198 or 898-1198. However, ASK1 does not promote the phosphorylation of GFP-HIPK2^{Δ583-798} due to the lack of protein complex formation.

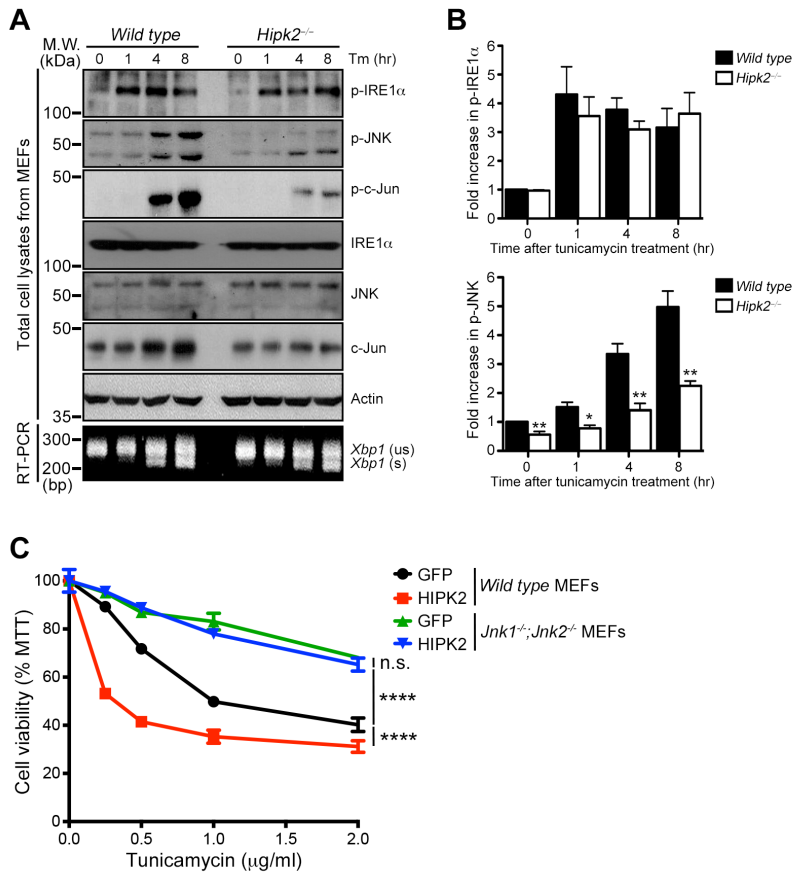


Figure S5. HIPK2-dependent JNK activation is impaired in *Hipk2*^{-/-} MEFs during ER stress, Related to Figure 2

(A-B) Protein lysates from *wild type* and *Hipk2*^{-/-} MEFs treated with tunicamycin for 0, 1, 4 and 8 hours were used in western blots to analyze the activation of IRE1 α , JNK, c-Jun and *Xbp1* mRNA splicing. Two-tailed unpaired Student's t test; ** indicates $p < 0.01$.

(C) *Wild type* and *Jnk1*^{-/-};*Jnk2*^{-/-} MEFs were transfected with GFP or GFP-HIPK2 and treated with tunicamycin to characterize the extent of cell death using MTT assays. 2 way ANOVA; **** indicates $p < 0.0001$.

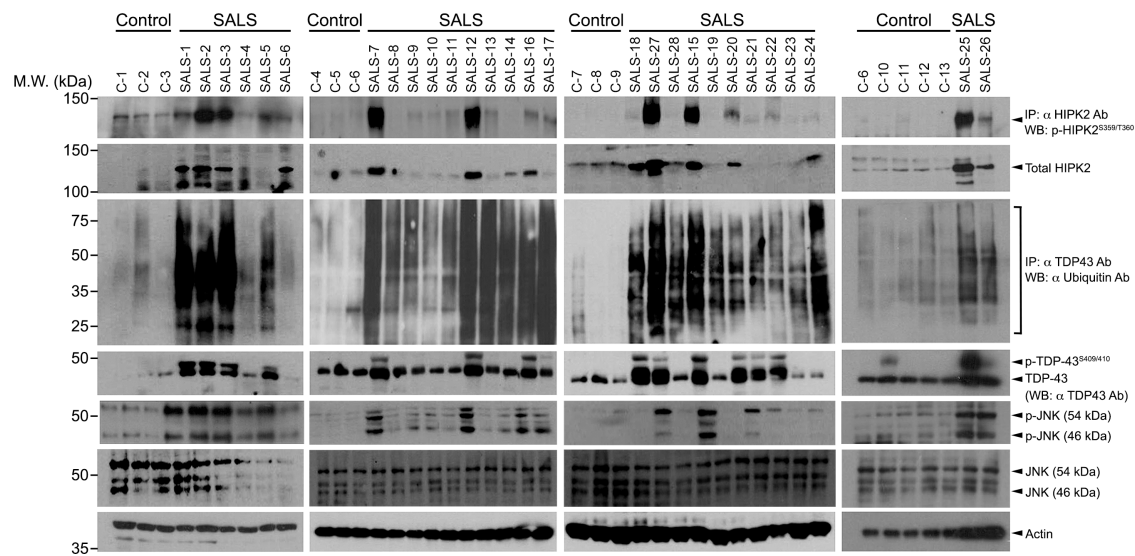


Figure S6. TDP-43 proteinopathy and activation of HIPK2-JNK pathway in sporadic ALS patients, Related to Figure 6

Western blot analyses of the spinal cord tissues from 13 controls with no history of neurological diseases and 28 cases of SALS. One gm of protein lysates from control and SALS cases were used to perform immunoprecipitation using α -HIPK2 or α -TDP-43 antibody, followed by western blot analyses using α -p-HIPK2 [S359/T360] or α -ubiquitin Ab, respectively. Western blot analyses of total HIPK2, p-TDP-43 [S409/410], p-JNK, JNK and actin were performed using 25-50 μ g of protein lysates.

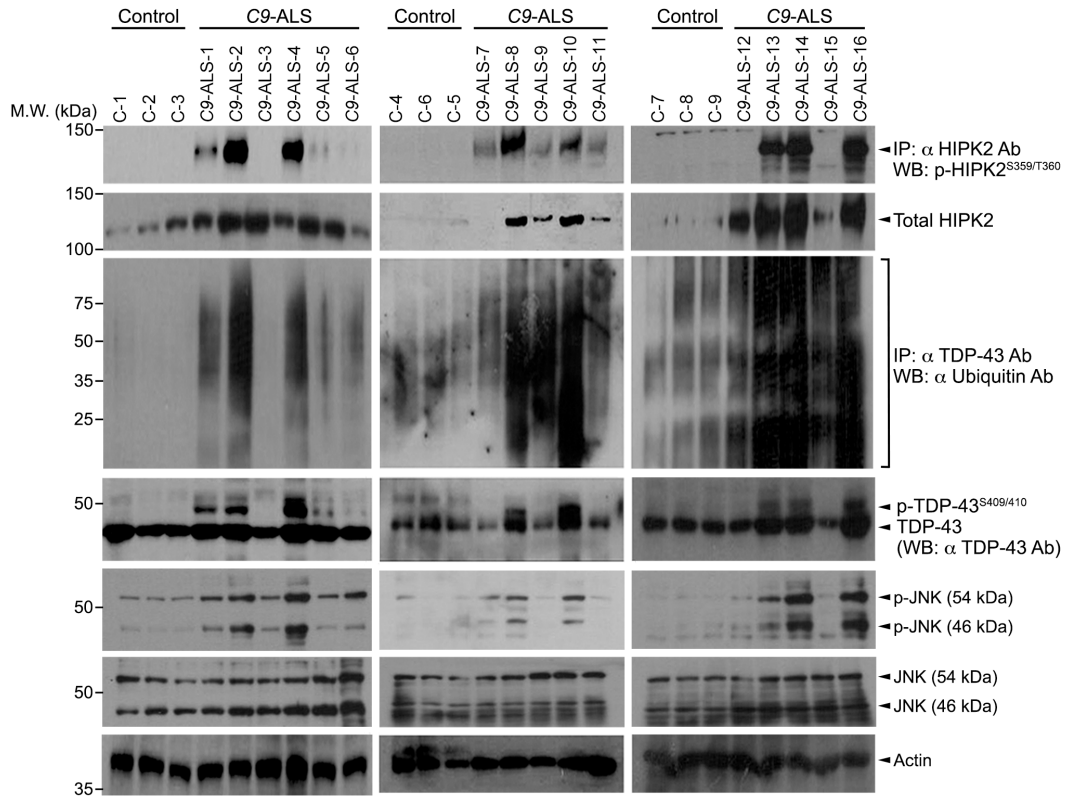


Figure S7. TDP-43 proteinopathy and activation of HIPK2-JNK pathway in familial ALS patients with C9ORF72 mutations, Related to Figure 6

Western blot analyses of the spinal cord tissues from 9 controls and 16 cases of C9-ALS. One gm of protein lysates from control and C9-ALS cases were used to perform immunoprecipitation using α -HIPK2 or α -TDP-43 antibody, followed by western blot analyses using α -p-HIPK2 [S359/T360] or α -ubiquitin Ab, respectively. Western blot analyses of total HIPK2, p-TDP-43 [S409/410], p-JNK, JNK and actin were performed using 25-50 μ g of protein lysates.

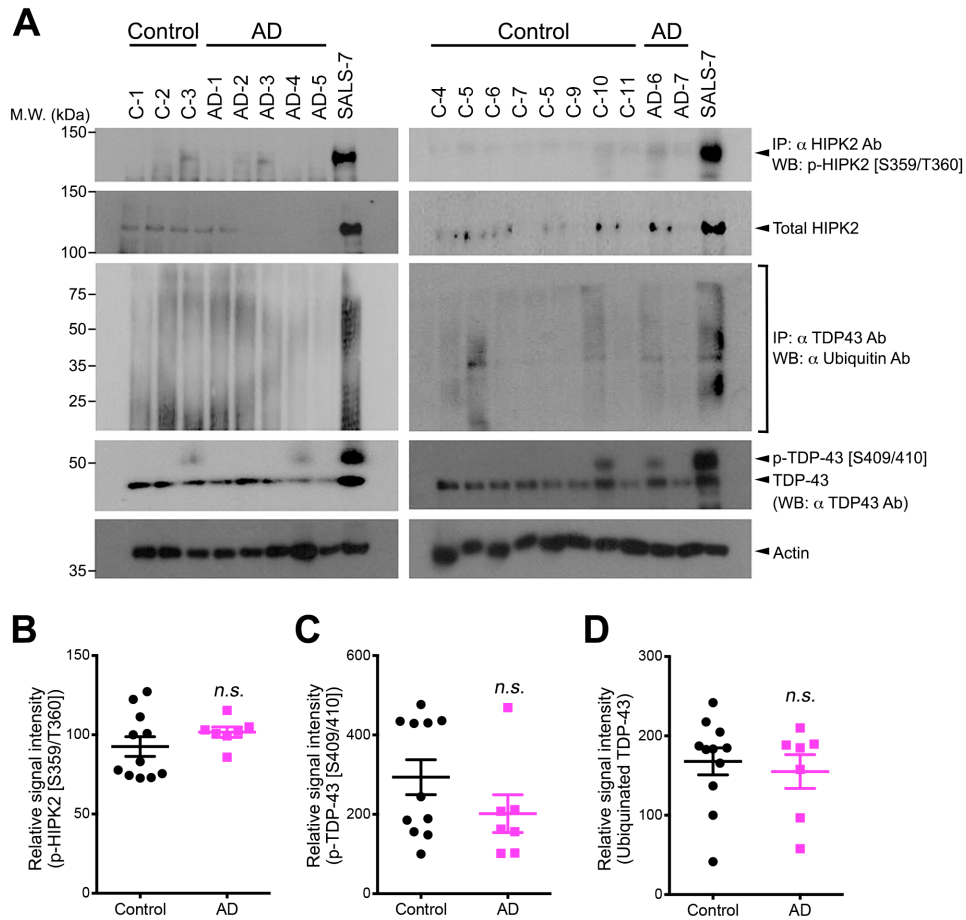


Figure S8. Lack of TDP-43 proteinopathy and activation of HIPK2-JNK pathway in Alzheimer's disease patients, Related to Figure 6

(A) Western blot analyses from the frontal cortex of 11 age-matched controls and 7 cases of Alzheimer's disease (AD). One gm of protein lysates from control and AD cases were used to perform immunoprecipitation using α -HIPK2 or α -TDP-43 antibody, followed by western blot analyses using α -p-HIPK2 [S359/T360] or α -ubiquitin Ab, respectively. Western blot analyses for total HIPK2, p-TDP-43 [S409/410] and actin were performed using 25-50 μ g of protein lysates.

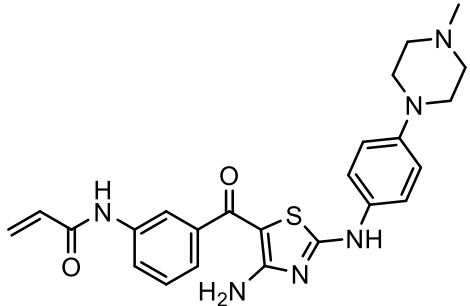
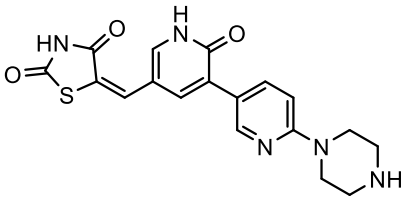
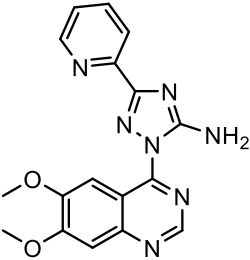
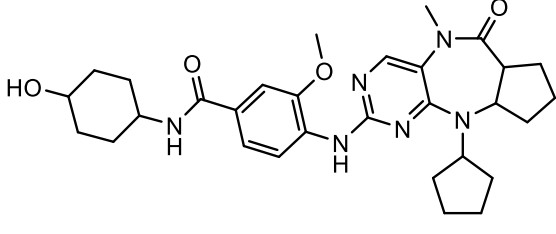
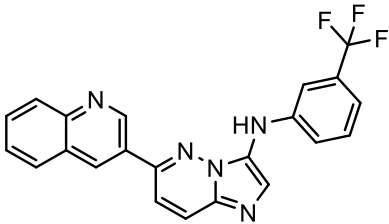
(B-D) Quantifications of p-HIPK2 [S359/T360], Ubiquitinated TDP-43 and ubiquitinated TDP-43 showed no difference between age-matched control and AD patient. Student's *t* test; n.s. indicates not significant.

Table S1 related to Figures 3 and 6. Summary of clinical and genetic information of human postmortem tissue samples.

| Case ID | Age at Death (yr) | Gender | PMI (hrs) | Clinical Diagnosis | C9ORF72 | Regions Examined | Neuropath Diagnosis |
|-------------|-------------------|--------|-----------|----------------------------|---------|------------------|---------------------|
| Control #1 | 63 | F | 28 | Infective endocarditis | -- | CSC | Control |
| Control #2 | 55 | F | 17 | Adenocarcinoma | -- | CSC | Control |
| Control #3 | 54 | F | 14 | Acute myeloid leukemia | -- | CSC | Control |
| Control #4 | 46 | F | 21 | Pneumonia | -- | CSC | Control |
| Control #5 | 72 | M | 14 | Pneumonia | -- | CSC | Control |
| Control #6 | 70 | M | 16 | Atherosclerosis | -- | CSC | Control |
| Control #7 | 14 | F | 24 | Pneumonia | -- | CSC | Control |
| Control #8 | 61 | F | 24 | Veno-occlusive disease | -- | CSC | Control |
| Control #9 | 7m | M | 18 | Wiskott-Aldrich syndrome | -- | CSC | Control |
| Control #10 | 55 | F | 28 | Pneumonia | -- | CSC | Control |
| Control #11 | 61 | F | 20 | Ovarian tumor | -- | CSC | Control |
| Control #12 | 94 | F | 22 | Myocardial infarction | -- | CSC | Control |
| Control #13 | 72 | M | 15 | Hypertensive heart disease | -- | CSC | Control |
| ALS #1 | 80 | M | 10.2 | SALS | -- | CSC | ALS |
| ALS #2 | 73 | M | 9.25 | SALS | -- | CSC | ALS |
| ALS #3 | 65 | F | 7.1 | SALS | -- | CSC | ALS |
| ALS #4 | 49 | M | 11.9 | SALS | -- | CSC | ALS |
| ALS #5 | 77 | M | 9.8 | SALS | -- | CSC | ALS |
| ALS #6 | 64 | M | 6 | SALS | -- | CSC | ALS |
| ALS #7 | 72 | M | 24 | SALS | -- | CSC | ALS |
| ALS #8 | 65 | M | 25 | SALS | -- | CSC | ALS |
| ALS #9 | 54 | F | 16 | SALS | -- | CSC | ALS |
| ALS #10 | 61 | M | 9 | SALS | -- | CSC | ALS |
| ALS #11 | 55 | F | 6 | SALS | -- | CSC | ALS |
| ALS #12 | 64 | M | 16 | SALS | -- | CSC | ALS |
| ALS #13 | 51 | M | 16 | SALS | -- | CSC | ALS |
| ALS #14 | 72 | F | 11 | SALS | -- | CSC | ALS |
| ALS #15 | 78 | M | 5.5 | SALS | -- | CSC | FTLD-TDP |
| ALS #16 | 78 | M | 5.5 | SALS | -- | CSC | ALS |
| ALS #17 | 76 | M | 23 | SALS | -- | CSC | FTLD-TDP |
| ALS #18 | 51 | F | 4 | SALS | -- | CSC | ALS |
| ALS #19 | 61 | M | 9 | SALS | -- | Unknown | ALS |
| ALS #20 | 58 | M | 24 | SALS | -- | Unknown | ALS |
| ALS #21 | 73 | M | 18.5 | SALS | -- | Unknown | ALS |
| ALS #22 | 72 | F | 6 | SALS | -- | Unknown | ALS |

| | | | | | | | |
|---------|----|---|-----|------------------------|-----------|---------|---------|
| ALS #23 | 73 | M | 12 | SALS | -- | Unknown | ALS |
| ALS #24 | 62 | M | 5.5 | SALS | -- | Unknown | ALS |
| ALS #25 | 62 | F | 20 | SALS | -- | Unknown | ALS |
| ALS #26 | 42 | M | 8 | SALS | -- | Unknown | ALS |
| ALS #27 | 59 | F | 6 | SALS | -- | Unknown | ALS |
| ALS #28 | 48 | F | 18 | SALS | -- | Unknown | ALS |
| ALS #29 | 60 | M | 40 | C9-ALS | Expansion | CSC | ALS |
| ALS #30 | 70 | M | 23 | C9-ALS | Expansion | TSC | ALS |
| ALS #31 | 59 | F | 6 | C9-ALS | Expansion | CSC | ALS |
| ALS #32 | 58 | M | 11 | C9-ALS | Expansion | TSC | ALS |
| ALS #33 | 64 | M | 15 | C9-ALS | Expansion | CSC | ALS |
| ALS #34 | 42 | M | 6 | C9-ALS | Expansion | Unknown | ALS |
| ALS #35 | 57 | M | 6 | C9-ALS | Expansion | Unknown | ALS |
| ALS #36 | 54 | M | 20 | C9-ALS | Expansion | Unknown | ALS |
| ALS #37 | 56 | F | 11 | C9-ALS | Expansion | Unknown | ALS |
| ALS #38 | 54 | M | 4 | C9-ALS | Expansion | Unknown | ALS |
| ALS #39 | 54 | M | 21 | C9-ALS | Expansion | Unknown | ALS |
| ALS #40 | 69 | F | 21 | C9-ALS | Expansion | TSC | ALS |
| ALS #41 | 55 | F | NA | C9-ALS | Expansion | CSC | ALS |
| ALS #42 | 39 | M | 15 | C9-ALS | Expansion | Unknown | ALS |
| ALS #43 | 57 | M | 15 | C9-ALS | Expansion | CSC | ALS |
| ALS #44 | 54 | M | 20 | C9-ALS | Expansion | Unknown | ALS |
| C-1 | 63 | F | 24 | Infective endocarditis | -- | FC | Control |
| C-2 | 55 | F | 28 | Adenocarcinoma | -- | FC | Control |
| C-3 | 54 | F | 20 | Acute myeloid leukemia | -- | FC | Control |
| C-4 | 46 | F | 22 | Pneumonia | -- | FC | Control |
| C-5 | 70 | M | 15 | Atherosclerosis | -- | FC | Control |
| C-6 | 72 | M | 24 | Pneumonia | -- | FC | Control |
| C-7 | 61 | F | 24 | Veno-occlusive disease | -- | FC | Control |
| C-8 | 55 | F | 28 | Pneumonia | -- | FC | Control |
| C-9 | 61 | F | 20 | Ovarian tumor | -- | FC | Control |
| C-10 | 94 | F | 22 | Myocardial infarction | -- | FC | Control |
| AD-1 | 86 | M | 24 | AD | -- | FC | AD |
| AD-2 | 90 | F | 20 | AD | -- | FC | AD |
| AD-3 | 90 | M | 22 | AD | -- | FC | AD |
| AD-4 | 91 | M | 15 | AD | -- | FC | AD |
| AD-5 | 75 | M | 7.5 | AD | -- | FC | AD |
| AD-6 | 79 | M | 20 | AD | -- | FC | AD |
| AD-7 | 72 | F | 18 | AD | -- | FC | AD |

Table S2 related to Figures 7 and 8. Structure-activity relationships of HIPK2 inhibitors.

| Compound ID | Structure | SMILES* | % p-HIPK2 inhibition (at 1 μ M) | EC ₅₀ to suppress Tm toxicity** |
|--------------|-------------------------------------------------------------------------------------|-------------------------------------------------------------------------------------------------|-------------------------------------|--------------------------------------------|
| JWD-065 |  | <chem>CN1CCN(CC1)C1=CC=C(NC2=NC(N)=C(S2)C(=O)C2=CC=CC(NC(=O)C=C)=C2)C=C1</chem> | 88.45% | 0.641 μ M |
| A64 |  | <chem>O=C1NC(=O)\C(S1)=C/C1=CNC(=O)C(=C1)C1=CC=C(N=C1)N1CCNCC1</chem> | 80.03% | 0.403 μ M |
| CP466722 |  | <chem>COC1=C(OC)C=C2C(=C1)N=CN=C2N1N=C(N=C1N)C1=NC=CC=C1</chem> | 55.10% | --*** |
| B28 |  | <chem>COC1=C(NC2=NC=C3N(C)C(=O)[C@H]4CCCC[C@H]4N(C4CC(C4)C3=N2)C=CC(=C1)C(=O)N1CCC(O)CC1</chem> | 40.05% | --*** |
| CVM-05-145-3 |  | <chem>FC(F)(F)C1=CC(NC2=CN=C3C=CC(=NN23)C2=CN=C3C=CC=C3=C2)=CC=C1</chem> | 40.87% | --*** |

* SMILES = Simplified molecular-input line-entry system. ** Tm = tunicamycin treatment at 1 μ g/ml. *** indicates that this compound did not protect HEK293 cells from tunicamycin toxicity.

SUPPLEMENTAL EXPERIMENTAL PROCEDURES

Motor Neuron Isolation and Motor Neuron Cultures

Primary motor neurons were isolated from E15.5 rat embryo spinal cords using previously described protocols (Camu and Henderson, 1992). Spinal cords were dissected and dissociated following incubation in 0.25% trypsin (Gibco). Motor neurons were isolated via immunopanning. Cells were incubated in a series of two negative selection plates (rat neural antigen, RAN2; galactocerebroside, GC) and one positive selection plate, p75NTR. Adherent neurons were re-suspended in growth medium consisting of DMEM (Gibco), B-27 (Life Tech), N-2 (Life Tech), Pen-Strep (Gibco), insulin (Sigma), forskolin (EMD), N-acetyl-L-cysteine (Sigma), BDNF, CNTF and GDNF (PeproTech). Motor neurons were routinely cultured on Matrigel-coated coverslips in 24-well plates at a density of 10^4 neurons/coverslip.

Cell Culture and Transfections

HEK293 cells and mouse embryonic fibroblasts (MEFs) were maintained in DMEM (Thermo Scientific) supplemented with 10% FBS (Gibco). *Wild type* and *Hipk2*^{-/-} MEFs were described previously (Shang et al., 2013; Wei et al., 2007). *Jnk1*^{-/-}; *Jnk2*^{-/-} MEFs were from Dr. Scott Oakes of University of California San Francisco. Primary cortical neurons were prepared from E15.5 mouse embryos and placed in MEM supplemented with 10% FBS, 1X penicillin/streptomycin, and 2mM glutamine (Gibco). On DIV 2, 5 μ M 5-Fluoro-2'-deoxyuridine (Sigma) was added to the cultures and, from DIV3, the primary cortical neurons were maintained in Neurobasal medium with B-27 supplement (Invitrogen). Transient transfection was performed using Lipofectamine 2000

(Invitrogen) according to manufacturer's instruction. For MTT cell viability assays in primary cortical neurons, electroporation was used for higher transfection efficiency. Electroporation was carried out using BioRad XCell Genepulser in 0.4 cm gap cuvettes (165-2081) for 2×10^6 cortical neurons mixed with 20 μg DNA in 400 μl Opti-MEM.

Reagents and Plasmids

Point mutations involving single or double amino acid substitution in HIPK2 were carried out using QuikChange Site-Directed Mutagenesis Kit (Stratagene) and confirmed by DNA sequencing. Tunicamycin and brefeldin A were purchased from Sigma-Aldrich (T7765 and B7651). All the siRNAs used for in this study were from Santa Cruz biotechnology (sc-39050, sc-29748). Wild type and mutant SOD1 constructs were provided by Dr. Scott Oakes (UCSF), and Human TDP-43 constructs (Myc-hTDP-43-WT and hTDP-43^{G348C}-Myc-His) and mouse TDP-43 constructs (mTDP-43^{A315T}-Myc-His, mTDP-43^{A90V}-Myc-His and mTDP-43^{M337V}-Myc-His) were provided by Dr. Gang Yu (UT Southwestern).

HIPK2 *In Vitro* Kinase Assays

HIPK2 was immunoprecipitated with anti-HIPK2 antibody (C-15) from total cell lysates prepared in IP lysis buffer (20 mM Tris, pH 8, 100 mM NaCl, 10% Glycerol, 0.5% NP-40, 2 mM EDTA, 100 mM NaF, 1 mM Na₃VO₄) supplemented with protease inhibitor cocktail and the incubated in a kinase buffer (25 mM Tris-HCl, pH 8, 10 mM MgCl₂) containing 5 μCi [γ -³²P] ATP (Perkin-Elmer) for 4 hours at room temperature. The samples were extensively washed in 10 mM Tris-HCl (pH 7.5) before proteins were

eluded from the resins by boiling in 2X protein sample buffer (20% Glycerol, 5% β -mercaptoethanol, 5% SDS, 250mM Tris pH 6.7, 0.05% bromophenol blue). Eluted samples were applied onto SDS pages and exposed on X-ray films (Clinic select blue).

Western Blot Analyses

Total cell lysates were prepared from cultured cells in NP-40 lysis buffer (1% NP-40, 20 mM Tris, pH 7.6, 150 mM NaCl, 100 mM NaF, 1 mM Na_3VO_4) supplemented with protease inhibitor cocktail. RIPA buffer (0.1% SDS, 1% sodium deoxycholate, 1% NP-40, 20 mM Tris, pH 7.6, 150 mM NaCl, 100 mM NaF, 1 mM Na_3VO_4) supplemented with protease inhibitor cocktail was used for protein extraction from tissues. Proteins in cell lysates were separated by SDS-PAGE and transferred to the PVDF membrane (Millipore). The membrane was blocked in 3% BSA before incubated with primary antibodies overnight at 4°C. Antibodies to p-ASK1 (3765, RRID: AB_2139929), p-JNK (9255, RRID: AB_2235013), p-c-Jun (9164, RRID: AB_2129578), JNK (9252, RRID: AB_2250373), c-Jun (9165, RRID: AB_2129578), HA-tag (2367, RRID: AB_2314619) were from Cell Signaling. Actin antibody (CP01) was from Calbiochem and activated caspase 3 antibody used in the Western blot in Figure 1Y was from R&D Systems (AF835). Ubiquitin antibody was from Abcam (ab122, RRID: AB_298927). Human and mouse TDP-43 were detected by anti-TDP-43 antibody (12892-1-AP [RRID: AB_2200505], 10782-1-AP [RRID: AB_615042], both from Proteintech Group). GFP antibody was from Aves Labs (GFP-1020, RRID: AB_10000240). HIPK2 antibody was purchased from Santa Cruz Biotechnology (sc-10294, RRID: AB_2117731) or Abcam (ab28507, RRID: AB_732895). Anti MEKK1 antibody was from Santa Cruz

Biotechnology (1-9C-2A, sc-449). p-IRE1 α was from Novus Biologicals (100-2323, RRID: AB_1109057). Epitope specific phosphorylated HIPK2 antibody was generated by immunizing rabbits with phospho-HIPK2 peptide (YenZyme Antibodies, LLC, South San Francisco). The membranes were washed with 0.1% TBST washing buffer followed by incubation with secondary antibodies conjugated with horseradish peroxidase. The Western blots were developed by ECL Chemiluminescence (Thermo scientific).

RT-PCR for *Xbp1* mRNA Splicing and Detection of *Hipk2* cDNA in MTT Assays

Total RNA was extracted using Trizol reagent (Invitrogen) according to manufacturer's instructions. 2 mg of total RNA was converted to cDNA by reverse transcriptase (Promega). For PCR reactions, following primers were used: *Hipk2* (forward: 5'-CCT ACC TTA CGA GCA GAC CAT-3'; reverse: 5'-CTT GCC CGG TGA CAG AAG-3'), murine *Xbp-1* (forward: 5'-TTA CGG GAG AAA ACT CAC GGC-3'; reverse: 5'-GGG TCC AAC TTG TCC AGA ATG C-3'), and human *Xbp-1* (forward: 5'-TTA CGA GAG AAA ACT CAT GGC-3'; reverse: 5'-GGG TCC AAG TTG TCC AGA ATG C-3'). PCR products were visualized by GelRed dye (Biotoum) on 2.5% Agarose gel.

Co-immunoprecipitation

Cell lysates were prepared in IP lysis buffer (20mM Tris, pH 8, 100mM NaCl, 10% Glycerol, 0.5% NP-40, 2mM EDTA, 100mM NaF, 1mM Na₃VO₄) supplemented with protease inhibitor cocktail and pre-cleared with protein A/G agarose for 1 hour. 500 μ g proteins were incubated with primary antibodies overnight at 4°C followed by additional

incubation with 30 μ l of protein A/G agarose (Santa Cruz Biotechnology) for 2 hours. After extensive washes in IP lysis buffer, proteins were eluded by boiling in 2X protein sample buffer (20% Glycerol, 5% β -mecaptoethanol, 5% SDS, 250 mM Tris, pH 6.7, 0.05% bromophenol blue). The supernatant was used for subsequent Western blot analysis.

Mass Spectrometry Analysis of Tunicamycin-induced HIPK2 Phosphorylation

HIPK2 was immunoprecipitated from HEK293 cells (RRID: CVCL_0045) expressing GFP-tagged HIPK2 (HIPK2-GFP) using anti-GFP antibodies coupled to magnetic beads (Abcam, ab193983, RRID: AB_1859750) as described in **Figure 2**. On-bead trypsin digest following reduction and alkylation was performed as previously described (http://msf.ucsf.edu/trypsin_digest.html). The digest samples were desalted with 0.2 μ L C18 ZipTips (Millipore, ZTC18M096) according to the manufacturer's protocol and resuspended in 12 μ L of 0.1% formic acid for MS analysis. LC-MS/MS was performed on a Waters NanoAcquity UPLC system (Waters, USA) online with an LTQ-Orbitrap Velos mass spectrometer (Thermo Fisher Scientific). Five μ L of each sample were injected onto a 25 cm EasySpray C18 column (Thermo Fisher Scientific) and separated by low-pH reverse phase chromatography over a 120 min gradient from 2% to 50% acetonitrile in 0.1% formic acid. The LTQ Orbitrap Velos instrument was operated in data-dependent mode to automatically switch between full scan MS and MS/MS acquisition using an HCD top 6 method. Survey MS spectra from m/z 250–1500 were acquired in the Orbitrap with resolution of 30,000 and target ion intensity of 1e6. Six most intense precursor ions with charge states greater than 1+ were sequentially

isolated to a target value of $3e4$ and fragmented in the HCD collision cell with normalized collision energy of 40%. The fragmentation spectra were detected in the Orbitrap with resolution of 7,500. Peak lists were created using Thermo Proteome Discoverer v1.4 (Thermo Fisher Scientific) which were then searched in Protein Prospector v5.14.0 (Baker et al., 2011) against the human SwissProtein database (Bairoch and Apweiler, 2000) downloaded on 09/16/2015 and corresponding random concatenated decoy database with the following parameters: up to two allowed missed cleavage sites, Carbamidomethyl-C constant modification, default variable modifications plus phosphorylation at STY, up to 3 modifications per peptide, SLIP score of >6 , and 20 ppm precursor mass and fragment mass accuracy. False discovery rate of $<1\%$ was used as the cutoff for peptide expectation values.

Stereomicroscopic Cell Counting

NeuN positive cortical neurons on 50 μm brain sections were counted using optical fractionator based unbiased method using Stereo Investigator software on PC that is attached to microscope with a motorized XYZ stage (MBF Bioscience, Williston, VT)(Zhang et al., 2007).

MTT Cell Viability Assay & LDH Cell Toxicity Assay

Cell viability was measured by 3-(4, 5-dimethylthiazol-2-yl)-2, 5-diphenyltetrazolium-bromide (MTT) reduction assay. 10^4 cells plated in a 96 well plate were incubated with 250 μM MTT. The converted dye was dissolved in 0.04 M HCl and 1% Triton-x-100 in absolute isopropanol. Optical density was measured at 560 nm using fluorescent

microplate reader. Cell toxicity was also determined by lactate dehydrogenase (LDH) release in culture medium using CytoTox 96R Non-Radioactive Cytotoxicity Assay kit (Promega) according to manufacturer's instruction. Briefly, cell culture medium from 96-well plate was incubated with reconstituted substrate mix for 30 minutes. The reaction was terminated by adding stop solution and the absorbance was determined at 490 nm using fluorescent microplate reader.

Intraperitoneal Injection of Tunicamycin

Three month-old *wild type* and *Hipk2^{-/-}* mice received a single sublethal intraperitoneal injection of tunicamycin (1 or 2 mg/kg) or DMSO, which was previously shown to robustly activate ER stress in kidneys (Zinszner et al., 1998). Four days after the injection, brains and spinal cords from these mice were collected for histological examination to determine the extent of neuronal cell death in the sensorimotor cortex and in cervical spinal cord. For biochemical analyses, fresh brain tissues were collected *wild type* and *Hipk2^{-/-}* mice at 1, 2, 3 or 4 days after tunicamycin injection.

Immunohistochemistry for Activated Caspase 3 and Terminal Deoxynucleotidyl

Transferase dUTP Nick End Labeling (TUNEL) Assay

Apoptotic neurons were detected by immunohistochemistry for activated caspase 3 or TUNEL assay for fragmented DNA. For immunohistochemistry, neurons fixed with 2% PFA were permeabilized with 0.2% Triton X-100 in PBS for 15 minutes. After quenching with 0.2 M Glycine for 15 minutes twice and blocking with 5% Goat serum and 5% BSA, the neurons were incubated overnight with 1:200 anti-activated caspase 3

(Cell Signaling, #9661, RRID: AB_331441) along with either 1:1000 Neu-N (Chemicon), or 1:1000 ChAT (Millipore). For TUNEL assay, fragmented DNA was detected using TACS2 TdT-Fluor *In Situ* Apoptosis detection Kit (Trevigen, Gaithersburg, MD) as manufacturer's instruction. Briefly, cells on coverslips were fixed with 3.7% PFA and permeabilized with cytonin for 30 mins. Incorporation of biotinylated nucleotides into fragmented DNA is visualized by Streptavidin-fluorescein conjugates and the images were collected by confocal microscopy.

Human Brain and Spinal Cord Tissues

Protein lysates from human tissues were prepared using the previously published protocols (Neumann et al., 2006). Briefly, 0.2 cm cross sections of spinal cord weighing ~0.1 gm were extensively washed on a shaker with ice-cold washing buffer (20 mM Tris pH 7.6, 100 mM NaF, 1mM Na₃VO₄, and proteinase inhibitor cocktail (Roche)) in 6 well plates. After a brief mincing with dissecting scissors, total proteins were extracted in 300 µl lysis buffer (1% NP-40, 20 mM Tris pH 7.6, 150 mM NaCl, 100 mM NaF, 1 mM Na₃VO₄, and proteinase inhibitor cocktail) using tissue grinding pestle (Kimble Chase). 1 mg of proteins were used for immunoprecipitation with α -HIPK2 Ab or α -TDP43 Ab, followed by western blot analyses with α -p-HIPK2 [S359/T360] Ab or α -ubiquitin Ab, respectively. Western blots were performed using 25 or 50 µg proteins, depending on the signal intensities.

HIPK2 Protein Quantification by Immunohistochemical and Immunofluorescent Microscopy

To quantify HIPK2 and misfolded SOD1^{G93A} protein expression in rodents (**Figure 2A-I**), we performed double immunofluorescent staining using HIPK2 (Santa Cruz Biotechnology, sc-10294) and C4F6 antibodies (provided by Dr. Daryl Bosco), which were detected using secondary antibodies conjugated with Alexa 568 and Alexa 488, respectively, in cervical spinal cord sections from P60 and P90 control and SOD1^{G93A} mice. Confocal images of HIPK2 and C4F6 were captured using a 60x objective on Nikon C2 microscope, and imported into NIH ImageJ to calculate Corrected Total Cell Fluorescence (C.T.C.F., expressed as arbitrary units [a.u.]) for the relative abundance of HIPK2 and misfolded SOD1^{G93A} proteins by drawing areas of interest in motor neurons. To quantify HIPK2 and misfolded SOD1 mutant proteins in 5 FALS cases with SOD1 mutations (SOD1^{E100G}, SOD1^{I113T}, SOD1^{G93A}, SOD1^{V14M}, and SOD1^{A4T}, n=200 motor neurons) and 3 age-matched controls (n=52 motor neurons)(**Figure 2L-P**). We performed two-color DAB IHC using HIPK2 and C4F6 antibodies in order to circumvent the high autofluorescent signals from lipofuscin in human spinal motor neurons. First, the HIPK2 IHC was developed using nickel ammonium sulfate enhancement technique to highlight HIPK2 proteins in the nuclei (dark blue color). Second, IHC using C4F6 antibody was detected by conventional DAB procedures to detect misfolded SOD1 mutant proteins (in brown color). Images of bright field two-color HIPK2-C4F6 IHC staining were captured using an Olympus BX53 microscope with identical parameters. Images were imported into NIH ImageJ and the chromagen intensity for HIPK2 and mutant SOD1 proteins was quantified using the methods described in <http://www.nature.com/protocolexchange/protocols/2931#/figures>. The same approach was used to quantify HIPK2 protein expression in the spinal motor neurons of control,

12 SALS cases (n=461 motor neurons) and 4 C9-ALS cases (n=168 motor neurons)(**Figure 6M-P**).

Mouse Behavior Tests

Rotarod test was performed to test motor coordination functions. Briefly, 3 trials per day on 2 consecutive days with 20-minute intervals on the accelerating rod (3 to 40 RPM in 5 minutes). Mean times on the rod were plotted over the trials.

Statistics

Data were analyzed by two-tailed Student's *t* test for pairwise comparisons or two-way ANOVA for multiple comparisons using Prism (GraphPad Software, San Diego, CA). All data were expressed as mean \pm SEM and *p* values of less than 0.05 were considered to be statistically significant, whereas *p* values greater than 0.05 were considered non-significant (n.s.).

REFERENCES

- Bairoch, A., and Apweiler, R. (2000). The SWISS-PROT protein sequence database and its supplement TrEMBL in 2000. *Nucleic Acids Res* 28, 45-48.
- Baker, P.R., Trinidad, J.C., and Chalkley, R.J. (2011). Modification site localization scoring integrated into a search engine. *Mol Cell Proteomics* 10, M111 008078.
- Camu, W., and Henderson, C.E. (1992). Purification of embryonic rat motoneurons by panning on a monoclonal antibody to the low-affinity NGF receptor. *J Neurosci Methods* 44, 59-70.
- Neumann, M., Sampathu, D.M., Kwong, L.K., Truax, A.C., Micsenyi, M.C., Chou, T.T., Bruce, J., Schuck, T., Grossman, M., Clark, C.M., *et al.* (2006). Ubiquitinated TDP-43 in frontotemporal lobar degeneration and amyotrophic lateral sclerosis. *Science* 314, 130-133.
- Shang, Y., Doan, C.N., Arnold, T.D., Lee, S., Tang, A.A., Reichardt, L.F., and Huang, E.J. (2013). Transcriptional corepressors HIPK1 and HIPK2 control angiogenesis via TGF-beta-TAK1-dependent mechanism. *PLoS Biol* 11, e1001527.
- Wei, G., Ku, S., Ma, G.K., Saito, S., Tang, A.A., Zhang, J., Mao, J.H., Appella, E., Balmain, A., and Huang, E.J. (2007). HIPK2 represses beta-catenin-mediated transcription, epidermal stem cell expansion, and skin tumorigenesis. *Proc Natl Acad Sci U S A* 104, 13040-13045.
- Zhang, J., Pho, V., Bonasera, S.J., Holtzman, J., Tang, A.T., Hellmuth, J., Tang, S., Janak, P.H., Tecott, L.H., and Huang, E.J. (2007). Essential function of HIPK2 in TGFbeta-dependent survival of midbrain dopamine neurons. *Nat Neurosci* 10, 77-86.
- Zinszner, H., Kuroda, M., Wang, X., Batchvarova, N., Lightfoot, R.T., Remotti, H., Stevens, J.L., and Ron, D. (1998). CHOP is implicated in programmed cell death in response to impaired function of the endoplasmic reticulum. *Genes Dev* 12, 982-995.